

# Some observations on filter pressing and sintering of yttria-stabilized zirconia nanopowder

Łukasz Zych\*, Krzysztof Haberko

*Faculty of Materials Science and Ceramics, AGH-University of Science and Technology,  
al. Mickiewicza 30, Cracow 30-059, Poland*

Available online 24 May 2006

## Abstract

The aim of this work was investigation of the sintering behaviour of a material prepared by filter pressing of an yttria-stabilized zirconia powder with grain sizes of about 8 nm. The water suspension of the powder was filter-pressed under 5 MPa. The early shrinkage of the filter-pressed sample, during its non-isothermal sintering was attributed to removal of water layers adsorbed on the powder surface. The observation of the microstructure evolution in samples heat-treated at different temperatures was performed. Pore growth during sintering was related both to presence of agglomerates, and to pore coalescence. Particle arrangement in the material was very uniform, which led to uniform densification of the material. Heat treatment of the sample for 30 min at 1200°C resulted in the material of 99.96% relative density, and grains within nanometric range.

© 2006 Elsevier Ltd. All rights reserved.

**Keywords:** Shaping; Sintering; Suspensions; ZrO<sub>2</sub>; Nanopowder

## 1. Introduction

Today one of the most rapidly developing fields of knowledge is nanotechnology. One of the parts of this broad field are nanomaterials, i.e. materials with one or more dimensions in the range of 1–100 nm (powders, layers or bulk materials). Properties of such materials can be significantly different from the behaviour of the ordinary ones, e.g. nanocrystalline ceramics, mainly oxides, shows superplastic behaviour.<sup>1</sup> Nanocrystalline ceramic materials are usually produced by compaction and subsequent sintering of nanopowders, which in turn are often produced by means of chemical wet powder preparation techniques, which lead to nanometric particles of very narrow size distribution. Nowadays, it is possible to obtain nearly all ceramic materials in the form of nanometric powders, but their shaping and sintering, which would lead to the dense material with nanometric grains, is still a challenge. The key to obtain such material is in the homogenous particle packing in the green body. Uniform packing of nanopowders by dry pressing needs extremely high pressures of the order of GPa, which are necessary to overcome huge friction forces acting between so fine particles.<sup>2,3</sup> These shaping conditions cause many technological problems,

such as limited size of a compacted body or internal stresses leading to the body cracking. The uniform packing of nanometric particles can be achieved by means of one of colloidal techniques e.g. slip casting, or centrifugal casting.<sup>4,5</sup> In the presence of a liquid phase which wets the nanometric particles and penetrates between them, the particles move more easily, which leads to their more uniform arrangement. The subject of colloidal processing of nanometric ceramic particles has not been broadly studied yet, and most of existing works concentrates on particles larger than 10 nm.<sup>5–7</sup>

The aim of the work was the investigation of sintering process of samples prepared by means of pressure filtration of a solid solution nanometric powder containing 3 mol% Y<sub>2</sub>O<sub>3</sub> and 97 mol% ZrO<sub>2</sub>, and particle size of about 8 nm.

## 2. Experimental

The 3 mol% yttria-doped zirconia powder was prepared by the hydrothermal treatment of X-ray amorphous co-precipitated gel of a given composition. The mutual solution of ZrOCl<sub>2</sub> and YCl<sub>3</sub> was introduced into ammonia water solution. The co-precipitated gel was washed with distilled water in order to remove NH<sub>4</sub>Cl, which interferes with the sintering process, and then hydro-thermally treated at 250 °C for 4 h under an autogenous water vapour pressure.<sup>8</sup> The specific surface area

\* Corresponding author. Tel.: +48 12 617 39 40; fax: +48 12 633 46 30.  
E-mail address: [lzych@agh.edu.pl](mailto:lzych@agh.edu.pl) (Ł. Zych).

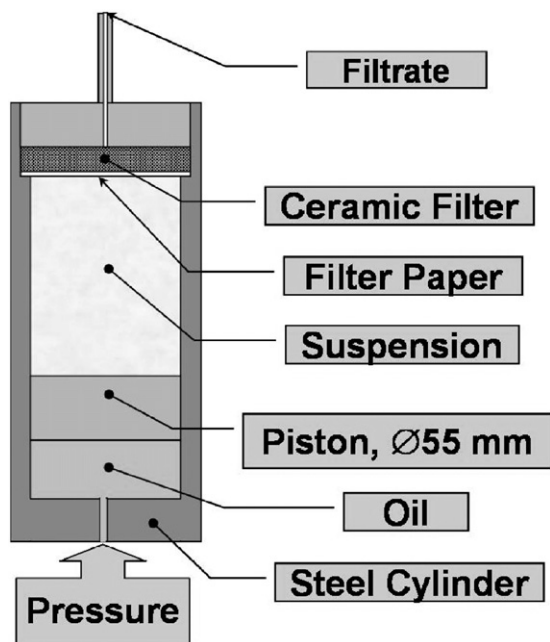


Fig. 1. Schematic drawing of the pressure filtration apparatus.

of the powder, and partially sintered samples was measured using BET method (Sorpt 1750, Carlo Erba Ins.) and their phase composition, and crystallite size were investigated by X-ray diffraction method (Cu K $\alpha$ , X'Pert Pro, Philips) using the Scherrer formula, and the powder was observed under TEM microscope (AEM CM 20, Philips). The average particle size of the powder was about 8 nm. The powder was kept in a water suspension of about 5 vol% concentration. The suspension was moulded using filter-pressing technique in the apparatus shown in Fig. 1. The suspension was forced by a steel piston (55 mm diameter) through a ceramic filter covered with filter paper. Pressure was increased up to 5 MPa, and kept constant until no water leakage was observed. The samples were carefully dried up to the constant weight in a desiccator over silica gel. The green density of the samples was estimated using GeoPyc 1360 apparatus (Micromeritics). The samples were non-isothermally sintered up to 1200 °C in dilatometer (with heating rate of 6 °C/min), and isothermally heat-treated at temperatures ranging from 100 to 1200 °C. Temperature was increased with 6 °C/min rate to a predetermined level, and then kept constant for 30 min. The samples' apparent density was measured by the Archimedes' method, pore size distribution was evaluated by the mercury porosimetry (Porosimeter 2000, Carlo Erba Ins.), and the microstructure was observed under TEM microscope, and SEM microscope (Leo 1530).

### 3. Results and discussion

#### 3.1. Powder characteristics

The obtained powder had a very narrow particle size distribution, which is characteristic of powders produced by hydrothermal technique, and it showed specific surface area of 130 m<sup>2</sup>/g.

Particle size calculated on the basis of this value was 8.1 nm. The value was close to the mean particle size assessed from transmission electron microphotographs (7.5 nm), and the one calculated from the X-ray diffraction line broadening (8.6 nm). It indicates that, although in case of nanopowders some level of agglomeration is inevitable, in our powder no broad contacts between particles were formed. In order to prevent the formation of strong bonds between particles, the powder was kept in a water suspension.

#### 3.2. Shaping process

The suspension concentration was about 9 vol%, and it was the maximum concentration allowing it to show liquid-like behaviour. At higher volume concentrations distances between nano-particles are so small that attractive forces cause their bonding, which leads to the formation of a rather stiff body. The original suspension had pH 7, which is close to the isoelectric point of the yttria-stabilized zirconia powder suspensions, which means that the suspension was flocculated. The suspension was filter pressed under 5 MPa. This pressure level was based on our previous investigations, which showed that samples moulded under higher pressures tend to crack during drying.

#### 3.3. Sintering process

Fig. 2 shows shrinkage of the filter-pressed sample versus temperature; on the same picture the sintering curve of a sample made by uniaxial dry pressing of a submicron powder of the same composition, manufactured by TOSOH Co., is also presented. Relative green density of both samples was similar, and close to 40%.

In case of the sample made of nanopowder, shrinkage starts at temperature as low as 150 °C, and up to this temperature the sample thermally expands. The early onset of the shrinkage can be attributed to the removal of the water layers adsorbed on the powder surface. This assumption is supported by the calculation based on the specific surface area of the powder, the amount of adsorbed water (determined by the thermogravimetric method), which showed that each particle is covered with a

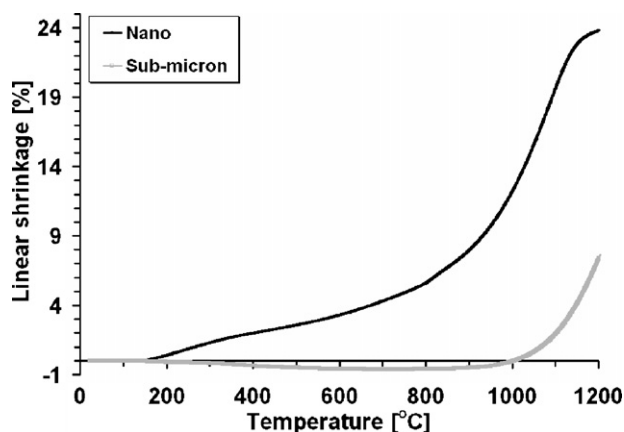


Fig. 2. Linear shrinkage of samples during non-isothermal sintering with the heating rate of 6 °C/min.

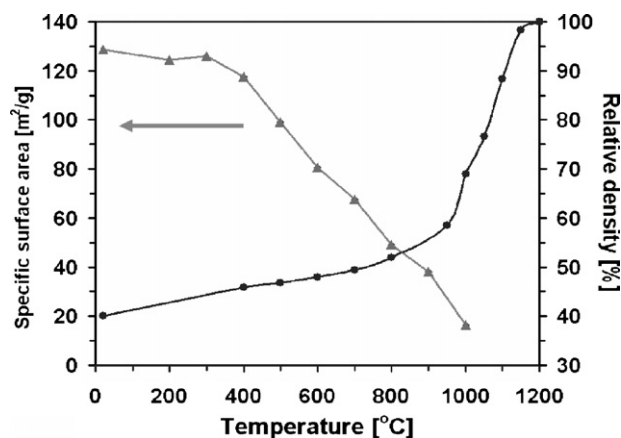


Fig. 3. Specific surface area, and relative density vs. temperature.

0.2 nm thick layer of adsorbed water. Considering the particle size ( $\sim 8$  nm), and green density of the samples ( $\sim 40\%$ ), the amount of water layers along a unit length can be estimated. Removing this amount of water leads to the shrinkage of about 2%, which is close to the observed value at about  $500^\circ\text{C}$ . The shrinkage nearly terminates at about  $1200^\circ\text{C}$ . Contrary to this behaviour, the sample made of a submicron, commercial, powder starts to shrink at about  $1000^\circ\text{C}$ . Fig. 3 presents density of samples heated up to pre-selected temperatures in the range  $100$ – $1200^\circ\text{C}$ , and held at each temperature for 30 min. The green density was about 40%, and the sample heat-treated at  $1200^\circ\text{C}$  reached 99.9% TD. The figure presents also the specific surface area change versus temperature. The particle diameter calculated on its basis is shown on Fig. 4., together with the crystallite size estimated on the basis of the X-ray diffraction line broadening. The good agreement between these values exists up to about  $500^\circ\text{C}$ , at higher temperatures particle size calculated from specific surface area becomes larger than the crystallite size, which indicates that intercrystallite boundaries are formed.

This figure presents pore sizes distribution in the samples heat-treated at indicated temperatures. The total pore volume decreases with temperature, which is obvious, but simultaneously a mean pore size increases. Pore growth usually accompanies densification and can be attributed to two factors.<sup>9</sup> One

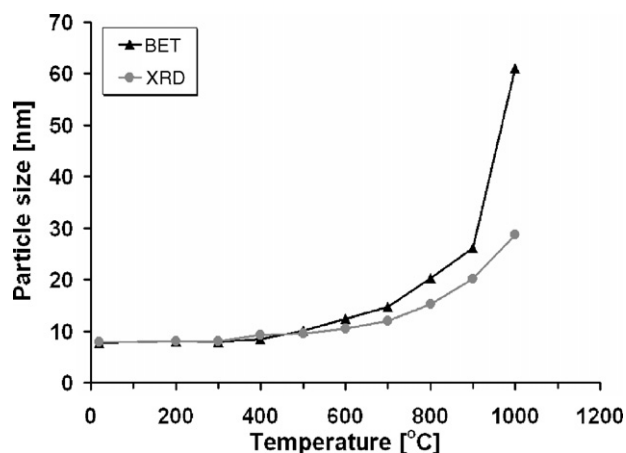


Fig. 4. Estimated particle size vs. temperature.

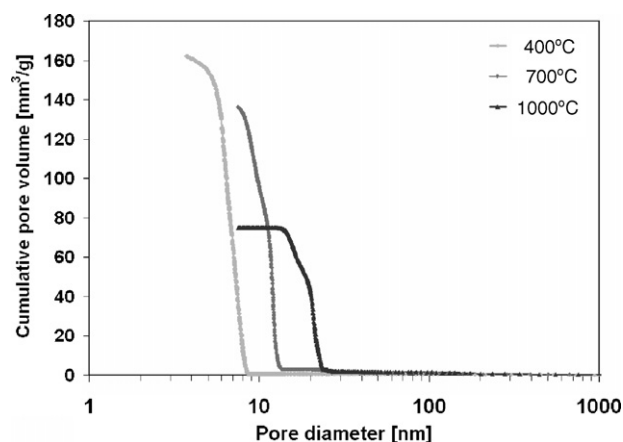


Fig. 5. Open porosity evolution.

is related to the occurrence in the green body areas differing in packing density. The denser areas originate from the powder of agglomerates which survive the shaping process. Within these areas porosity disappears faster than in the areas of lower density, causing essential increase of the pore sizes in the latter ones. Under usually applied sintering conditions such pores do not disappear. The next reason of pore growth is related to the grain growth. Under conditions of a continuous grain growth, pores move with the grain boundaries. Coalescence of such pores is recorded as pore size increase.

If the latter of these two processes is dominating, pore sizes measured and calculated using a simple geometric relationship (1), should agree.

$$\frac{D_P}{D_g} = \sqrt[3]{\frac{V_P}{V_g}}, \quad (1)$$

where  $D_P$  is the pore size (modal pore size, porosimetry),  $D_g$  the grain size (crystallite size, XRD),  $V_P$  the volume fraction of pores, and  $V_g$  the volume fraction grains, respectively.  $V_g$  equals to relative density of the material (Fig. 3), and  $V_P = 1 - V_g$  (Fig. 5).

Fig. 6 illustrates the interrelation between measured and calculated pore sizes according to Eq. (1). Good correlation between measured and calculated pore sizes indicates that they are equal to each other. It points out that pore growth can be ascribed to the growth of crystallites.

Scanning electron micrographs reveal (Fig. 7) that a microstructure of the filter-pressed samples consists of agglomerates of nanometric size, which, according to the specific surface area data (Fig. 3), are porous. The agglomerates grow with temperature. Detailed analysis of the pore size distribution of the samples indicates that the distribution is bimodal. Probably the smaller pores belong to intra-agglomerate porosity, while larger ones are related to inter-agglomerate porosity.

It suggests that pore growth is caused by faster densification within agglomerates than between them. However, the pore coalescence mechanism can operate within agglomerates as well. The pore size distribution is very narrow, and both pore populations are located close to each other, so the presented earlier model of the pore growth is valid (Fig. 8).

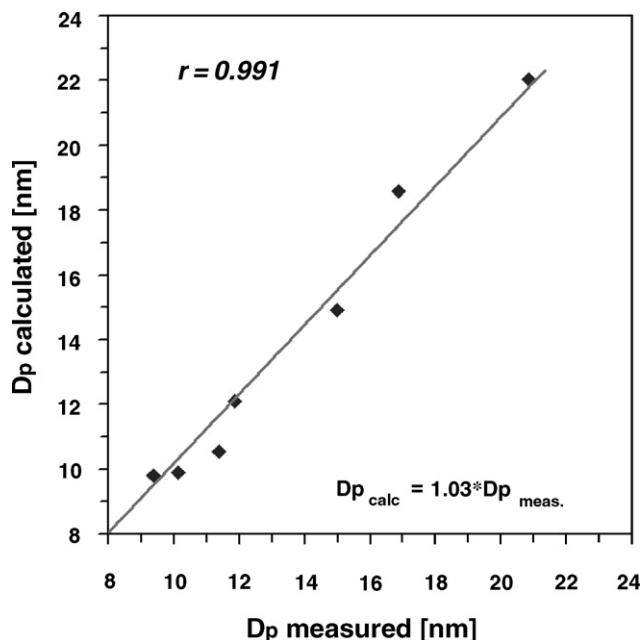


Fig. 6. Interrelation between measured and calculated pore size.

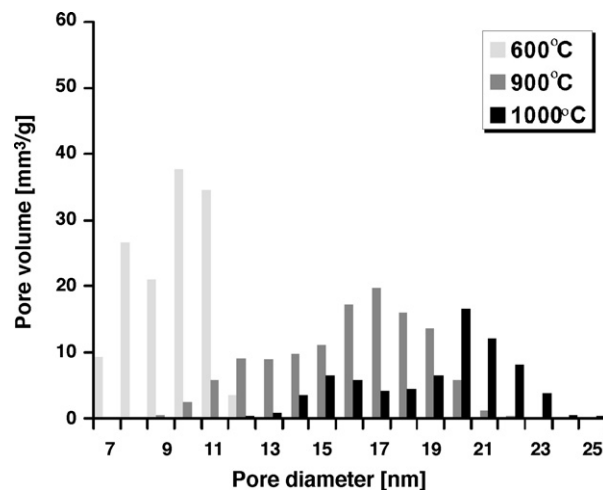


Fig. 8. Pore size distribution histograms of samples heat-treated at different temperatures.

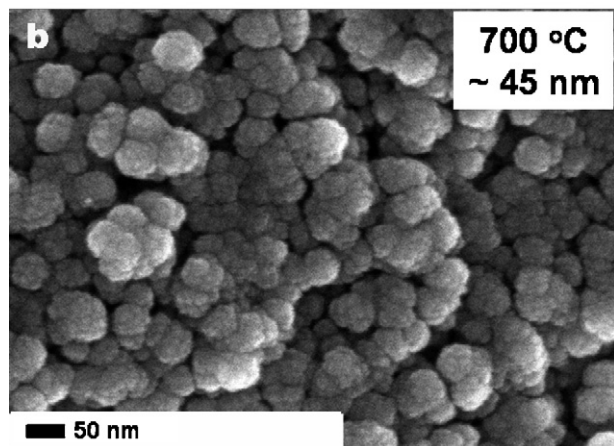
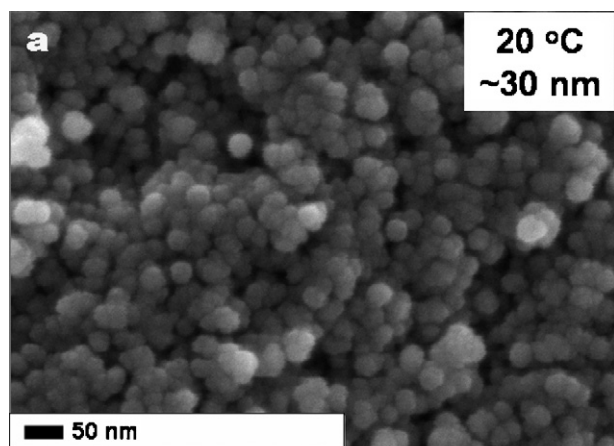


Fig. 7. Scanning electron micrographs of fracture surface of the filter pressed samples: (a) green sample, (b) sample heat-treated at 700 °C, 0.5 h. The mean agglomerate size is presented.

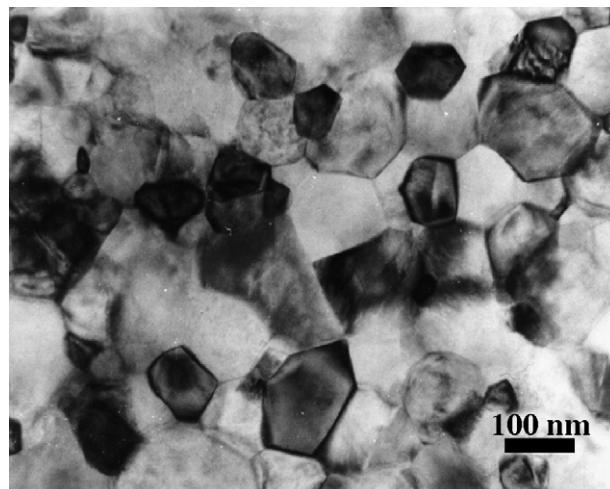


Fig. 9. Transmission electron micrograph of the sample sintered at 1200 °C for 0.5 h.

Although the agglomeration related pore growth exists, the pore size distribution remains narrow, and the pores are relatively small, which allows almost full densification of the sample (99.96%) at temperature 1200 °C. Such a low temperature limits grain growth, so the microstructure of this sample consists of grains in nanometric range (Fig. 9), i.e. the modal grain size estimated on the basis of TEM microphotographs was 108 nm, and about half of grains are smaller than this value.

#### 4. Summary

Application of the filter-pressing method for the shaping of water suspension of nanometric (mean particle size 8 nm) zirconia powder resulted in green samples with homogenous particle arrangement and a very narrow pore size distribution. Its sintering at 1200 °C for 0.5 h led to a dense material (99.9% TD) with modal grain size about 100 nm.

## Acknowledgement

The work was financially supported by the Polish State Committee for Scientific Research under grant No.3 T08D 017 27

## References

1. Hunt, W. H., Nanomaterials: nomenclature, novelty, and necessity. *JOM*, 2004, **56**, 13–18.
2. Mayo, M. J., Processing of nanocrystalline ceramics from ultrafine particles. *Int. Mater. Rev.*, 1996, **41**, 85–115.
3. Gao, L., Li, W., Wang, H. Z., Zhou, J. X., Chao, Z. J. and Zai, Q. Z., Fabrication of nano Y-TZP materials by superhigh pressure compaction. *J. Eur. Ceram Soc.*, 2001, **21**, 135–138.
4. Rhodes, J., Agglomeration and particle size effects on sintering of yttria-stabilized zirconia. *J. Am. Ceram. Soc.*, 1981, **64**, 19–21.
5. Uchikoshi, T., Sakka, Y., Ozawa, K. and Hiraga, K., Pressure filtration and sintering of fine zirconia powder. *J. Eur. Ceram. Soc.*, 1998, **18**, 669–674.
6. Liu, D.-M., Adsorption, rheology, packing, and sintering of nanosize ceramic powders. *Ceram. Int.*, 1999, **25**, 107–113.
7. Vasylykiv, O. and Sakka, Y., Synthesis and colloidal processing of zirconia nanopowder. *J. Am. Ceram. Soc.*, 2001, **84**, 2489–2494.
8. Pyda, W., Habeko, K. and Bucko, M. M., Hydrothermal crystallization of zirconia and zirconia solid solutions. *J. Am. Ceram. Soc.*, 1991, **74**, 2622–2629.
9. Kingery, W. D., Bowen, H. K. and Uhlmann, D. R., *Introduction to Ceramics*. John Wiley and Sons, New York, 1976.